Remarkable Turn-On and Color-Tuned Piezochromic Luminescence: Mechanically Switching Intramolecular Charge Transfer in Molecular Crystals

Qingkai Qi, Jingyu Qian, Xiao Tan, Jibo Zhang, Lijuan Wang, Bin Xu, Bo Zou, and Wenjing Tian**

The molecular crystals of acridonyl-tetraphenylethene (AD-TPE) exhibit an intriguing turn-on and color-tuned luminescence in response to mechanical grinding and hydrostatic compression. On the basis of in-depth experimental and computational studies, it is hypothesized that the origin of the piezochromic behavior from the D-phase to the B-phase is the change of the intramolecular geometrical conformation, especially for the torsion angle between the TPE and AD moiety. The different molecular conformation in the two distinctive solid phases causes the substantial switching of the intramolecular charge transfer (ICT) process, which can be directly correlated with the subsequent fluorescence from locally excited (LE) state and ICT state in both phases. The AD-TPE molecular system presents a very rare example of high-contrast reversible fluorescence tuning driven by a switching of the excited state in the solid state under the mechanical stimuli, and thus provides a novel mechanism of the piezochromic behavior.

1. Introduction

Piezochromic luminescent materials have been attracted intensive interests over the past decade due to their promising applications in optical storage, pressure sensors, rewritable media, and security ink.[1] A most promising approach for piezochromic luminescence is to regulate and control the molecular stacking mode of the luminescent molecules under the external mechanical stimulus,[2] which allows to achieve the reversibility and reproducibility of the piezochromic transition and to reduce the pressure required for the luminescent transition. But regulating and controlling the molecular stacking mode in the condensed phase sometimes suffers from the notorious aggregation caused quenching[3] effect, which result in a low contrast ratio in the luminescence recording.

High-contrast luminescence recording requires not only the obvious two-color luminescence switching, but also the dramatic switching in the luminescence intensity which is difficult to realize for the traditional piezochromic luminescent materials.[4] Recently, a few piezochromic materials with on–off or off–on luminescence property have been reported. Pei and co-workers[5] reported a turn-on luminescence of cocrystallized complex of 2,5-di(*E*)-distyrylfuran and *N*-alkyl-substituted maleimides by breaking the donor–acceptor (D–A) interaction after applying mechanical force. Park and co-workers[4b,6] found the mechanically controlled photoinduced electron transfer in molecular assemblies of dicyanodistyrylbenzene derivative with the obvious off–on luminescence, and shear-induced luminescence on–off switching in stilbenic π-dimer crystals by reversible [2 + 2] cycloaddition. Tang and co-workers[7] and Wang and co-workers[8] reported some crystallization-induced emission enhancement (CIEE) materials with on–off emission under grinding, respectively. In addition, Tang[9] reported the mechanical force induced off–on emission of the defect-sensitive crystals based on diaminomaleonitrile-functionalized Schiffbase. Almost all the above researches focused on the luminescence change under the mechanical grinding. However, the magnitude of the grinding force cannot be precisely controlled and the direction of the grinding force is anisotropic, which is difficult to investigate the mechanism of the piezochromic luminescence by mechanical grinding. Instead, the research of piezochromic luminescence under hydrostatic pressure is a more effective and controllable method to explore the piezochromic mechanism. Our group[10] and Yamaguchi group[11] have reported piezochromic luminescence of 9,10-bis((*E*)-2-(pyrid-2-yl)vinyl)anthracene and tetrathiazolylthiophene, respectively, which both showed gradually red-shifted wavelength and decreased intensity of luminescence due to the enhanced π–π interaction under the hydrostatic pressure.

Herein, a structurally well-defined donor–acceptor (D–A) molecule, AD-TPE (**Figure 1**a), incorporating a twisted TPE unit as an electron donor, and a rigid AD unit as an electron acceptor have been readily synthesized with high yield according to Scheme S1 (Supporting Information) via the C–N coupling

Dr. Q. Qi, J. Qian, J. Zhang, Dr. L. Wang, Prof. B. Xu, Prof. W. Tian
State Key Laboratory of Supramolecular Structure and Materials
College of Chemistry
Jilin University
Changchun 130012, P. R. China
E-mail: xubin@jlu.edu.cn; wjtian@jlu.edu.cn
Dr. X. Tan, Prof. B. Zou
State Key Laboratory of Superhard Materials
Jilin University
Changchun 130012, P. R. China

DOI: 10.1002/adfm.201501224

© 2015 WILEY-VCH Verlag GmbH & Co. KGaA, Weinheim

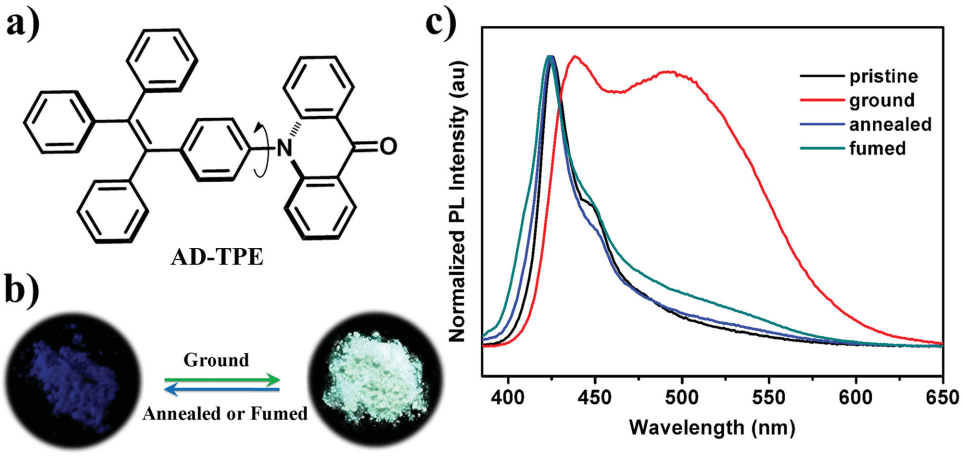

Figure 1. a) Structural formula of AD-TPE. b) Fluorescence images and c) corresponding fluorescence spectra of AD-TPE under different treatments.

reaction.[12] Unlike the traditional piezochromic materials with two luminescence color switching, the molecule shows an intriguing turn-on and color-tuned piezochromic luminescence in response to the mechanical grinding and the hydrostatic pressure. This mechanical stimuli responsive system with high-contrast luminescence may be found the practical applications in the optical recording and sensing. Furthermore, it offers an intriguing example for understanding the structure-property relationship of the solid-state luminescent materials under the mechanical stimuli. To gain deep insight into the intriguing luminescence turn-on and color-tuned behavior of AD-TPE molecule, we have comprehensively investigated the structural, optical and photophysical properties, combining with the theoretical calculations and stimulations.

2. Results and Discussion

The aggregates of AD-TPE were prepared by a simple precipitation method and exhibited a drastic increase of the fluorescence intensity comparing with the nonfluorescent THF solution (Figure S1, Supporting Information). The aggregates formed in 90% (fw) mixture were then checked by transition electron microscopy and dynamic light scattering (Figure S2, Supporting Information), which indicates that the nanoparticles are in amorphous state.

To our surprise, the AD-TPE pristine powders just have very weak emission under 365 nm UV light irradiation, which was called the dark-phase (D-phase), as shown in Figure 1b. But after being ground, AD-TPE powders show extremely bright cyan emission, which was called the bight-phase (B-phase). The difference between the emissions of the pristine and ground powders is sufficiently large as to be easily distinguished by the naked eyes. The fluorescent quantum yield Φ_F of AD-TPE powders presents a 43-fold enhancement from 0.01 to 0.43 before and after grinding (Table S1, Supporting Information). The emission of ground powders can recover to the initial D-phase after heating at 250 °C for 1 min or fuming with the organic solvent.

The powder X-ray diffraction (PXRD) measurement was performed to primarily understand the microstructure of the pristine powders treated under different conditions. The results show that AD-TPE forms different molecular stacking architectures before and after grinding–heating or solvent-fumed treatment (**Figure 2**a). These observations indicate that the molecular stacking converts from a well-order crystalline phase to an amorphous phase, i.e., from D-phase to B-phase, induced by grinding. Additionally, it should be noted that the DSC curve (Figure 2b) of the ground powders displays a cold-crystallization transition peak at 115 °C prior to melting at 328 °C, indicating that the ground powders present in a metastable amorphous phase and convert to a stable crystalline phase via an exothermal recrystallization process. The results further demonstrate that AD-TPE possesses metastable B-phase and stable D-phase in the aggregation state, and grinding leads to a change of the solid-state molecular aggregation mode from a stable ordered crystalline phase to a metastable amorphous phase, which significantly enhanced the luminescence efficiency and tuned the emission color.

The large single crystal of AD-TPE has been cultivated and obtained by slow solvent evaporation at room temperature from its ethanol/chloroform solutions, which enables further confirmation of the molecular structure by the crystallographic

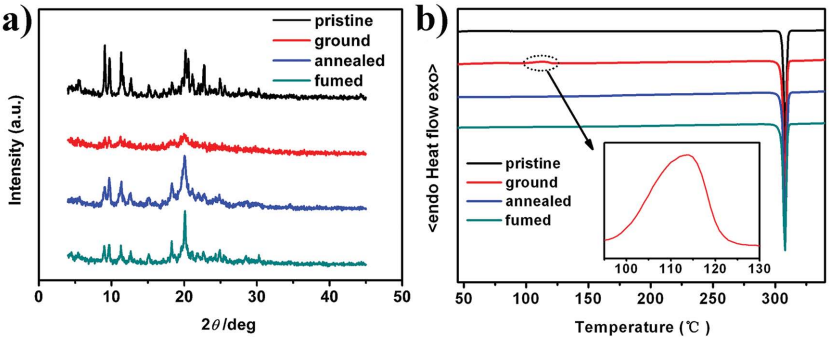

Figure 2. a) PXRD patterns and b) DSC curves of AD-TPE powders: pristine, ground and annealed sample (150 °C for 1 min) and fumed sample (fumed with ethyl acetate).

© 2015 WILEY-VCH Verlag GmbH & Co. KGaA, Weinheim

analysis (Table S3, Supporting Information). As prepared, they are colorless and transparent, and almost no emission under the UV illumination, just like the initial D-phase powders mentioned above. The simulated PXRD pattern from the AD-TPE crystal data was accorded well with the pattern of the initial powder (Figure S3, Supporting Information), suggesting that the D-phase was mainly composed of the microcrystals of AD-TPE.

Notably, the luminescence of AD-TPE single crystal can also be switched on under hydrostatic pressure. Hydrostatic pressure up to 3.00 GPa is applied by using a sapphire anvil cell technique, where silicone oil is used as a pressure-transmitting medium. During the compression process, the colorless and transparent single crystal become pale yellow and translucent, and the weak fluorescence gradually switch to the bright cyan. The visible and fluorescent images of the single crystal under different hydrostatic pressures, as well as the absorption and emission spectra, are shown in **Figure 3**. From Figure 3b,c, we can see that the change of the piezochromic luminescent process is not continuous, but there is an obvious two-step change process with the increase of the hydrostatic pressure. Initially, both the visible images and absorption spectra of the crystal have no obvious change (Figure 3a,d), but the fluorescence images (Figure 3b) became bright with no emission color change before the applied external pressure below 1.01 GPa. From the emission spectra of the crystal (Figure 3c), there is no new emission band, but the luminescence intensity gradually enhanced. With the increase of the applied pressure, a redshifted absorption and a new broad emission band at long-wavelength region concomitantly appear. Eventually, AD-TPE crystal shows a bright cyan emission at 2.98 GPa. The observed changes of both the emission intensity and wavelength of single crystal under hydrostatic pressure are similar with those of powders under grinding, implying that this unique piezochromism of AD-TPE under different mechanical stimuli may come from the same origin.

Although a few of fluorophores have been reported to show the switchable luminescence under the external stimuli, molecules that show such a unique remarkable turn-on and color-tuned luminescence with high-contrast characteristic under both shear force and hydrostatic pressure are rarely presented. First, the observed quenching emission in the initial D-phase and single crystal is quite different from the previous reports about other TPE derivatives in which the twisted conformation often provides a large steric hindrance and enhances the luminescence in aggregation state. In addition, the shear or hydrostatic-pressure-induced emission of AD-TPE shows not only remarkable enhanced intensity, but also a new and board emission band in the long-wavelength region. Compared to the emission and absorption spectra of the isolated AD-TPE monomer in solution, the observed new emission indicates that the different emitting states arise due to the excitation of distinctly different species in the ground state rather than the formation of excimers. Although the detailed mechanism of piezochromic luminescence modulation of the reported molecules is still unclear and is likely to vary from case to case,

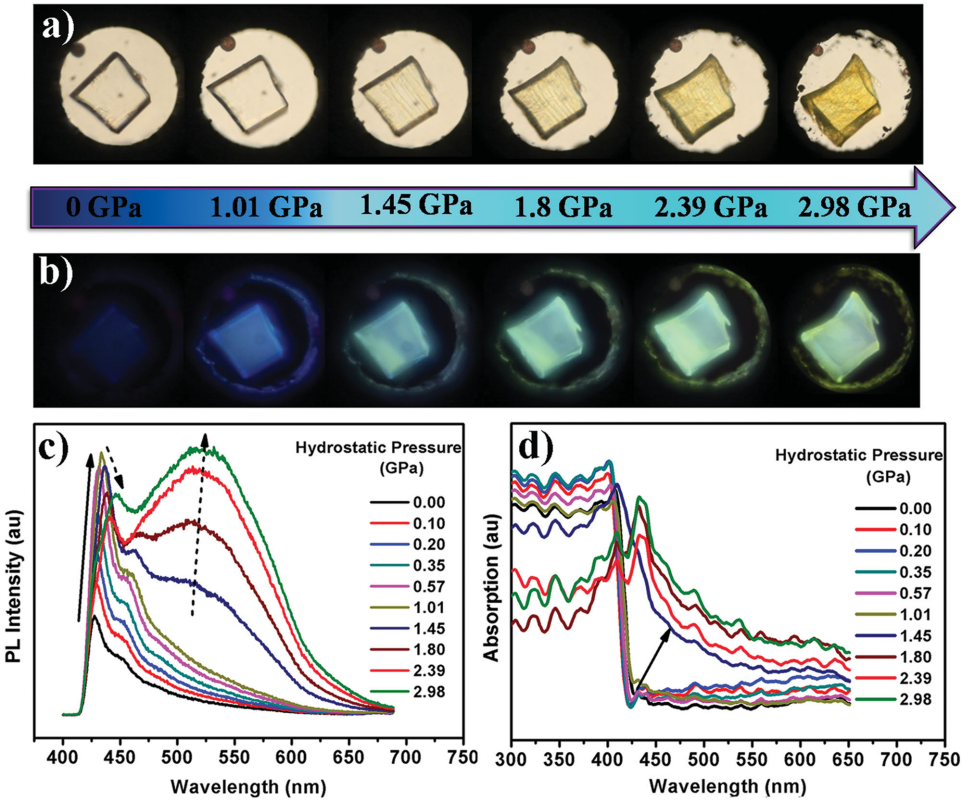

Figure 3. a,b) Visible and fluorescence images of a single crystal of AD-TPE under different hydrostatic pressures. c,d) Corresponding fluorescence and absorption spectra.

© 2015 WILEY-VCH Verlag GmbH & Co. KGaA, Weinheim

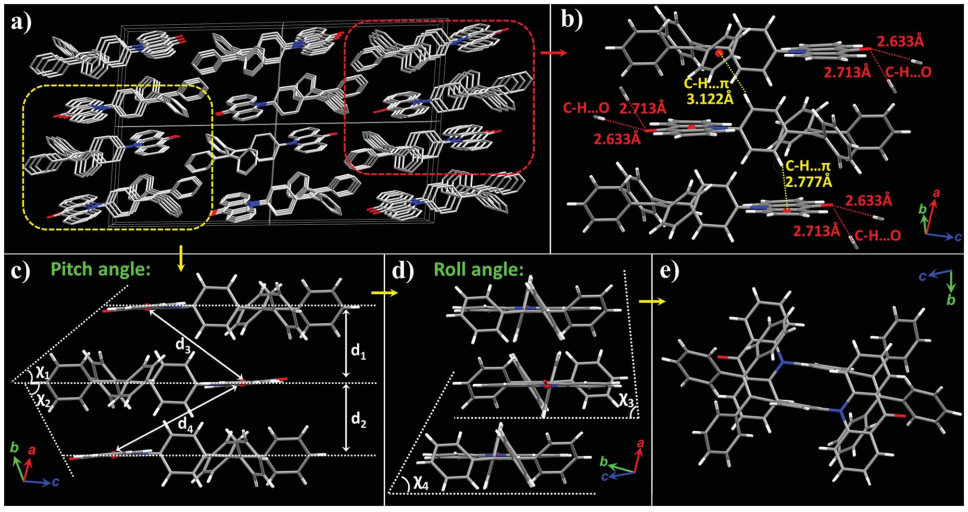

Figure 4. a) The packing pattern and b) weak interactions in the crystal. c) The distances between the whole molecule planes, the center distances between two AD units, the pitch angles, and d) roll angles of two H-aggregates. e) The perspective view of the dimers along the *a*-axis.

these observations appears to suggest that the unique piezochromic luminescence behavior of AD-TPE can be assigned to the switch of the excited state before and after the mechanical stimuli.

To explore the underlying origins of the quenched emission in the initial aggregation state and remarkable turn-on and color-tuned piezochromic luminescence, the structural analysis of AD-TPE single crystal was performed to establish the structure-property relationship. **Figure 4**a shows the molecular packing structure in the single crystal. Each unit cell consists of two independent molecules (Figure S4, Supporting Information). As shown in Figure S5 (Supporting Information), the dihedral angle between AD and the directly connected benzene ring of TPE approaches 75° which is much larger than the dihedral angles (about 55°) between the other three benzene rings of TPE and ethylene plane. As shown in Figure 4c and Table S4 (Supporting Information), the large distances (7.612 and 9.697 Å) between the ADs indicate that there is no face-to-face π–π interaction between the adjacent molecules. Besides, the increased steric hindrance by the twisted TPE unit affords the relatively loose packing in the crystal which could be easily amorphized under the mechanical stimulus and exhibit piezochromic luminescence.

Since the TPE unit is an electron donor while the AD unit acts as an electron acceptor, AD-TPE is a D–A molecule comprising one local dipole. The dipole moment is pointed from AD to TPE with a value about 7.27 D (Figure S6, Supporting Information). As illustrated in Figure 4, the strong dipole–dipole interaction places the central TPE unit of the upper sheet just above the AD unit of the lower sheet, bringing about the special dimers with the antiparallel and side-by-side alignment in the crystal. Besides, the crystal is constructed by the CH...O, CH...π interactions, which are summarized in Figure 4b. In spite of the large inter-plane distances (4.576 and 4.547 Å) between the adjacent molecules in the two dimmers, the strong dipole–dipole interaction is promoted by the small slip-arrangement with a pitch angle of 40° and 63° (Figure 4c and Table S4, Supporting Information) and a roll angle of 85° and 63° (Figure 4d and Table S4, Supporting Information), either along the long molecular axes or the short axes. It suggests that two kinds of H-type aggregates were formed in crystal. Comparing with the PL spectra in solution and polymethyl methacrylate (PMMA) film, the disappeared emission peak at around 399 nm of the powder indicated that the forbidden of exciton transition (0–0) from the second lowest excited state (S_2) to the ground state (S_0), which also demonstrated the formation of H-aggregates in the powders (Figure S7, Supporting Information). The structural analysis suggests that the weak emission from AD-TPE single crystal and the initial *D*-phase powders was attributed to the formation of H-aggregates through the strong dipole–dipole interaction and weak supramolecular interactions (Figure S8, Supporting Information).

To investigate the change of the molecular geometries and packing structure of AD-TPE under mechanical stimuli, we perform density functional theory (DFT) calculations by using the CASTEP module on the basis of the structure data of single crystal. The optimized lattice parameters, the distance between the two H-aggregates, and geometrical parameters under the external stress of 0, 1, 2, and 3 GPa are listed in Table S3–S5 (Supporting Information). These parameters indicate that the molecular geometries trend toward the planarization conformation and the molecular packing becomes tighter with the increase of the molecular density. Nevertheless, it should be noted that the changes of the geometrical parameters in the single crystal under the pressure consisted with the two stage processes of the piezochromic behavior. At the initial stage, the interplane distances and pitch angles of the two adjacent molecules in the dimers were greatly reduced with the increasing of applied external pressure. When further increasing the external pressure, the relative locations of the adjacent molecules show small variation and the adjacent molecules still keep the H-type arrangement. It is noted that comparing with the molecular packing, the molecular conformation, especially the dihedral angle (θ) between the AD group and the neighboring benzene ring changes pronouncedly from 75.56° to 70.89° (Table S5, Supporting Information). These changes suggest that the unique piezochromic behavior of AD-TPE should not

© 2015 WILEY-VCH Verlag GmbH & Co. KGaA, Weinheim

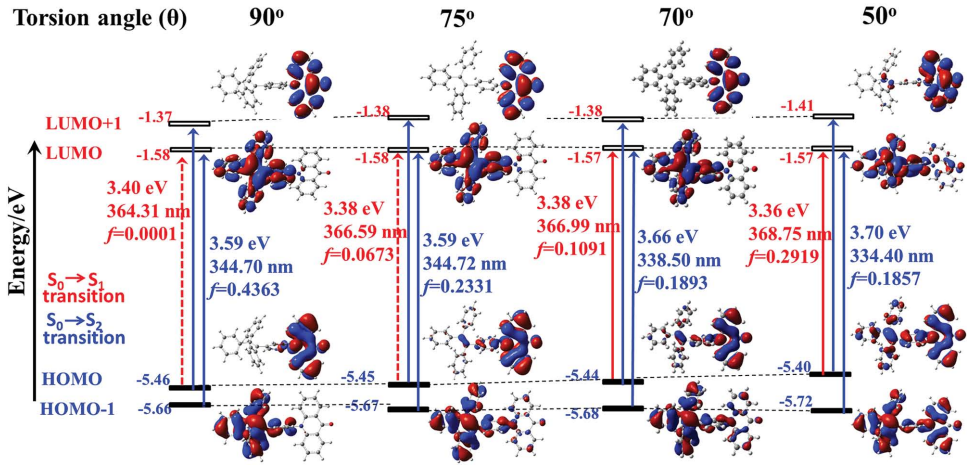

Figure 5. Energy diagrams and the frontier orbitals contribution of AD-TPE in fixed conformation based on the gradually decreased torsion angel (θ) between TPE and AD, and their lowest- and second-lowest-energy transitions estimated by TD-DFT calculations at the B3LYP/6-31G(d, p)** level.

originate from the transformation of the molecular aggregation mode, but may come from the change of the molecular conformation induced by mechanical stimuli.

The most significant electronic effect of the twist geometry of AD-TPE is the weak intramolecular charge transfer (ICT) property, and even frustrates the charge transfer between the donating TPE unit and accepting AD unit. Indeed, the optimized geometry of AD-TPE in the isolate state is almost orthogonal with a torsion angle of ca. 88.9° between TPE and AD unit, calculated using B3LYP/6-31G(d, p)** by Gaussian 09. However, AD-TPE shows no obvious solvatochromic effect (Figure S9, Supporting Information), which supposed that the emission of AD-TPE in solution may be assigned to the locally excited (LE) state, but not arise from the ICT state. From the electronic density distribution of molecular orbitals (MOs) of AD-TPE (Figure S10, Supporting Information), the largest electron coefficients in the HOMO are located along the AD moiety, whereas the coefficients in the LUMO are concentrated on the TPE unit, suggesting that the MOs almost separate completely between TPE and AD unit. It indicated that upon the photoexcitation there might be considerable LE state, which is further verified by the time-dependent (TD) DFT calculations. According to TD-DFT calculations in the gas phase (Table S6, Supporting Information), the lowest energy transition (HOMO → LUMO) of AD-TPE is symmetry-forbidden, while the higher energy transition (HOMO−1 → LUMO, HOMO → LUMO+1) is symmetry-allowed. The forbidden nature of $S_0 \rightarrow S_1$ transition is consistent with the weak fluorescent character of AD-TPE. Consequently, the transition is predicted to occur at a high energy level, regarded as the LE transition. It is in agreement with the absorption spectrum of AD-TPE in solution which is the superposition of the absorption spectra of TPE and AD monomer (Figure S11, Supporting Information). In addition, the emission spectra of AD-TPE monomer in solution and PMMA film is analogous to that of AD monomer in solution, further demonstrating that the emission of AD-TPE should be originated from the LE state.

As mentioned above, the emission property of AD-TPE shows a dependence on the change of torsion angle under the external mechanical stimuli. To explain why AD-TPE showed completely different characteristics in the electronic spectra when the torsion angle changed, the TD-DFT calculations for the model structure with different torsion angle were performed. The results are shown in **Figure 5**. It demonstrates that the HOMO → LUMO transition shows a dynamic switching from the symmetry forbidden to symmetry allowed transition with the torsion angle decrease, while the HOMO−1 → LUMO and HOMO → LUMO+1 transitions with higher energies are always allowed. In addition, the decrease of the torsion angle facilitates the delocalization of the nitrogen lone pair to the π system of the AD acceptor, leading to an overlap of the frontier orbitals and enhanced coplanarity between TPE and AD units. Owing to the increased overlap of the frontier orbitals, the electron density on HOMO is distributed across the full molecular skeleton, and that on LUMO mainly located at TPE moiety, indicating the formation of ICT state. These variations accompanying the decrease of the torsion angle, particularly the switching of the HOMO → LUMO transition, are consistent with the redshifted absorption spectra of AD-TPE. For example, the absorption spectra of ground powder and high-pressure crystal both show obvious redshift comparing with that of the pristine powder and crystal (Figure S12, Supporting Information and Figure 3d). The increased oscillator strength of ICT transition is also responsible for the long-wavelength emission band and increased radiative transition rate.

3. Conclusion

In summary, we have presented a novel luminescence molecule AD-TPE that exhibits the remarkable turn-on and color-tuned luminescence under mechanical grinding or hydrostatic compression. The almost orthogonal conformation between TPE and AD fully separates the electronic distribution and inhibits the ICT process, leading to the emission from LE state in the D-phase of the molecular crystals. The twisted conformation can be changed by the force perturbation when the molecule is under the mechanical stimuli, resulting in an overlap of the frontier orbitals between donor and acceptor and the formation of ICT state. Thus, the switching of excited state characteristics

© 2015 WILEY-VCH Verlag GmbH & Co. KGaA, Weinheim

by the mechanical stimuli induced the change in luminescence from the nonemission D-phase to the bright cyan emission B-phase. We anticipate that the concept of the mechanical switching of the excited state will inspire the development of a new class of piezochromic luminescent materials with high-contrast ratio, and further provide an important insight into the solid state luminescent properties of the twisted D-A molecules.

All experimental procedures are reported in the Supporting Information.

Supporting Information

Supporting Information is available from the Wiley Online Library or from the author.

Acknowledgements

This work was supported by 973 Program (Grant No. 2013CB834702), the Natural Science Foundation of China (Grant Nos. 21204027, 21221063, and 91227202), program for Chang Jiang Scholars and Innovative Research Team in University (Grant No. IRT101713018), and Graduate Innovation Fund of Jilin University (Grant No. 2014013).

Received: March 27, 2015
Revised: April 19, 2015
Published online: May 15, 2015

[1] a) Y. Sagara, T. Kato, *Nat. Chem.* **2009**, *1*, 605; b) A. L. Balch, *Angew. Chem. Int. Ed.* **2009**, *48*, 2641; c) Y. Sagara, S. Yamane, T. Mutai, K. Araki, T. Kato, *Adv. Funct. Mater.* **2009**, *19*, 1869; d) M. Kinami, B. R. Crenshaw, C. Weder, *Chem. Mater.* **2006**, *18*, 946; e) A. Pucci, F. D. Cuia, F. Signori, G. Ruggeri, *J. Mater. Chem.* **2007**, *17*, 783; f) A. Pucci, G. Riggeri, *J. Mater. Chem.* **2011**, *21*, 8282; g) M. Krikorian, S. Liu, T. M. Swager, *J. Am. Chem. Soc.* **2014**, *136*, 2952; h) Z. H. Guo, Z. X. Jin, J. Y. Wang, J. Pei, *Chem. Commun.* **2014**, *50*, 6088; i) B. Xu, Z. Chi, J. Zhang, X. Zhang, H. Li, X. Li, S. Liu, Y. Zhang, J. Xu, *Chem. Asian J.* **2011**, *6*, 1470; j) B. Xu, M. Xie, J. He, B. Xu, Z. Chi, W. Tian, L. Jiang, F. Zhao, S. Liu, Y. Zhang, Z. Xu, J. Xu, *Chem. Commun.* **2013**, *49*, 273; k) J. Wang, J. Mei, R. Hu, J. Z. Sun, A. Qin, B. Z. Tang, *J. Am. Chem. Soc.* **2012**, *134*, 9956; l) S. J. Yoon, J. W. Chung, J. Gierschner, S. K. Kim, M. G. Choi, D. Kim, S. Y. Park, *J. Am. Chem. Soc.* **2010**, *132*, 13675; m) G. Zhang, J. Lu, M. Sabat, C. L. Fraser, *J. Am. Chem. Soc.* **2010**, *132*, 2160; n) P. Zhang, W. Dou, Z. Ju, X. Tang, W. Liu, C. Chen, B. Wang, W. Liu, *Adv. Mater.* **2013**, *25*, 6112; o) Q. Qi, Y. Liu, X. Fang, Y. Zhang, P. Chen, Y. Wang, B. Yang, B. Xu, W. Tian, S. X. Zhang, *RSC Adv.* **2013**, *3*, 7996; p) Q. Qi, J. Zhang, B. Xu, B. Li, S. X. A. Zhang, W. Tian, *J. Phys. Chem. C* **2013**, *117*, 24997; q) J. Wu, H. Wang, S. Xu, W. Xu, *J. Phys. Chem. A* **2015**, *119*, 1303.

[2] a) N. Mizoshita, T. Tani, S. Inagaki, *Adv. Mater.* **2012**, *24*, 3350; b) H. Ito, T. Saito, N. Oshima, N. Kitamura, S. Ishizaka, Y. Hinatsu, M. Wakeshima, M. Kato, K. Tsuge, M. Sawamura, *J. Am. Chem. Soc.* **2008**, *130*, 10044; c) C. Löwe, C. Weder, *Adv. Mater.* **2002**, *14*, 1625; d) J. Kunzelman, M. Kinami, B. R. Crenshaw, J. D. Protasiewicz, C. Weder, *Adv. Mater.* **2008**, *20*, 119; e) Y. Sagara, T. Mutai, I. Yoshikawa, K. Araki, *J. Am. Chem. Soc.* **2007**, *129*, 1520; f) Y. Sagara, T. Komatsu, T. Ueno, K. Hanaoka, T. Kato, T. Nagano, *Adv. Funct. Mater.* **2013**, *23*, 5277; g) Z. Zhang, D. Yao, T. Zhou, H. Zhang, Y. Wang, *Chem. Commun.* **2011**, *47*, 7782; h) Y. Dong, J. Zhang, X. Tan, L. Wang, J. Chen, B. Li, L. Ye, B. Xu, B. Zou, W. Tian, *J. Mater. Chem. C* **2013**, *1*, 7554.

[3] J. B. Birks, *Photophysics of Aromatic Moelcules*, Wiley-VCH, London **1970**.

[4] a) W. Z. Yuan, Y. Tan, Y. Gong, P. Lu, J. W. Y. Lam, X. Y. Shen, C. Feng, H. H. Y. Sung, Y. Lu, I. D. Williams, J. Z. Sun, Y. Zhang, B. Z. Tang, *Adv. Mater.* **2013**, *25*, 2837; b) M. S. Kwon, J. Gierschner, S. J. Yoon, S. Y. Park, *Adv. Mater.* **2012**, *24*, 5487; c) Y. Gong, Y. Tan, J. Liu, P. Lu, C. Feng, W. Z. Yuan, Y. Lu, J. Z. Sun, G. He, Y. Zhang, *Chem. Commun.* **2013**, *49*, 4009; d) Y. Zhang, J. Sun, G. Zhuang, M. Ouyang, Z. Yu, F. Cao, G. Pan, P. Tang, C. Zhang, Y. Ma, *J. Mater. Chem. C* **2014**, *2*, 195.

[5] J. Luo, L. Y. Li, Y. Song, J. Pei, *Chem. Eur. J.* **2011**, *17*, 10515.

[6] J. W. Chung, Y. You, H. S. Huh, B. K. An, S. J. Yoon, S. H. Kim, S. W. Lee, S. Y. Park, *J. Am. Chem. Soc.* **2009**, *131*, 8163.

[7] X. Luo, J. Li, C. Li, L. Heng, Y. Q. Dong, Z. Liu, Z. Bo, B. Z. Tang, *Adv. Mater.* **2011**, *23*, 3261.

[8] X. Cheng, D. Li, Z. Zhang, H. Zhang, Y. Wang, *Org. Lett.* **2014**, *16*, 880.

[9] T. Han, Y. Hong, N. Xie, S. Chen, N. Zhao, E. Zhao, J. W. Y. Lam, H. H. Y. Sung, Y. Dong, B. Tong, B. Z. Tang, *J. Mater. Chem. C* **2013**, *1*, 7314.

[10] Y. Dong, B. Xu, J. Zhang, X. Tian, L. Wang, J. Chen, H. Lv, S. Wen, B. Li, L. Ye, B. Zou, W. Tian, *Angew. Chem. Int. Ed.* **2012**, *51*, 10782.

[11] K. Nagura, S. Saito, H. Yusa, H. Yamawaki, H. Fujihisa, H. Sato, Y. Shimoikeda, S. Yamaguchi, *J. Am. Chem. Soc.* **2013**, *135*, 10322.

[12] D. A. K. Vezzu, J. C. Deaton, M. Shayeghi, Y. Li, S. Huo, *Org. Lett.* **2009**, *11*, 4310.

© 2015 WILEY-VCH Verlag GmbH & Co. KGaA, Weinheim